Diversity and Distributions, (Diversity Distrib.) (2013) 19, 567–579

BIODIVERSITY RESEARCH

Mapping ecological risks with a portfolio-based technique: incorporating uncertainty and decision-making preferences

Denys Yemshanov[1]*, Frank H. Koch[2], Mark Ducey[3] and Klaus Koehler[4]

[1]*Natural Resources Canada, Canadian Forest Service, Great Lakes Forestry Centre, 1219 Queen Street East, Sault Ste. Marie, ON P6A 2E5, Canada,* [2]*USDA Forest Service, Southern Research Station, Eastern Forest Environmental Threat Assessment Center 3041 Cornwallis Road, Research Triangle Park, NC 27709, USA,* [3]*Department of Natural Resources and the Environment, University of New Hampshire, 114 James Hall, Durham, NH 03824, USA,* [4]*Canadian Food Inspection Agency, 59 Camelot Drive, Ottawa, ON K1A 0Y9, Canada*

*Correspondence: Denys Yemshanov, Natural Resources Canada, Canadian Forest Service, Great Lakes Forestry Centre, 1219 Queen Street East, Sault Ste. Marie, ON P6A 2E5, Canada.
E-mail: dyemshan@nrcan.gc.ca

ABSTRACT

Aim Geographic mapping of risks is a useful analytical step in ecological risk assessments and in particular, in analyses aimed to estimate risks associated with introductions of invasive organisms. In this paper, we approach invasive species risk mapping as a portfolio allocation problem and apply techniques from decision theory to build an invasion risk map that combines risk and uncertainty in a single map product.

Location Canada.

Methods We divide the study area into a set of spatial domains and treat each domain as an individual 'portfolio' with a unique distribution of the expected impacts of invasion. The risk of invasion is then mapped by finding nested 'efficient' portfolio sets that identify the geographic areas exhibiting the worst combinations of the estimated risk of invasion and the uncertainty in that estimate. For Canadian municipalities, we apply the approach to quantify the risk that a given location will receive invasive forest pests with commercial freight transported via the North American road network. We compare risk allocation techniques that employ the concepts of nested mean-variance (M-V) frontiers and second-degree stochastic dominance.

Results While both methods based on M-V and the stochastic dominance principles identified similar areas of highest risk, they differed in how they demarcated moderate-risk areas. Furthermore, they address uncertainty in different ways, treating it as a risk premium (in the case of nested M-V frontiers) or producing risk-averse delineations (in the case of stochastic dominance).

Main conclusions The portfolio-based approach offers a viable strategy for dealing with the typically wide variability in risk estimates caused by a lack of knowledge about a new invader. The methodology also provides a tractable way of incorporating decision-making preferences into the final risk estimates and thus better aligns risk assessments with particular decision-making scenarios about the organism of concern.

Keywords

Epistemic uncertainty, human-assisted spread, invasibility, mean-variance frontier, road network, stochastic dominance.

INTRODUCTION

Geographic mapping of risks is a common exercise in many environmental disciplines, for example, the analysis of flooding (Büchele *et al.*, 2006; FEMA, 2003) or environmental hazards (Briggs, 2000), and in particular, in assessing the risks of invasive species (Boender *et al.*, 2007; Magarey *et al.*, 2009; Venette *et al.*, 2010). In general terms, 'pest risk mapping' can be described as the prioritization of geographic domains facing the threat of establishment of a non-native organism (Koch *et al.*, 2009; Yemshanov *et al.*, 2009a; Magarey *et al.*, 2011). The geographic area of concern is divided into

DOI: 10.1111/ddi.12061
http://wileyonlinelibrary.com/journal/ddi

A Journal of Conservation Biogeography
Diversity and Distributions
Special Issue: Risks, decisions, and biological conservation

a set of small units, so each element can be prioritized by the potential for the invader to be established and cause damage to a host resource.

Risk maps use a variety of metrics, such as the likelihood of the pest's arrival (Koch *et al.*, 2011; Yemshanov *et al.*, 2012a) or projected resource losses (Borchert *et al.*, 2007; Yemshanov *et al.*, 2009b), to describe the estimated risk of pest invasion. The choice of risk metric is often operationally driven. For example, if a risk map is used to guide early detection, then a metric related to introduction is probably more relevant than one measuring impact (Magarey *et al.*, 2009; Venette *et al.*, 2010). Frequently, the measure of risk is translated into an ordinal-scale variable (i.e. a rank) which, in turn, is used to identify the decision-making priorities in the geographic area of interest (FHTET, 2007a,b).

When knowledge about an invasive organism is poor (a typical situation for alien species), the measures of risk tend to be depicted in coarse, 'high–low' terms (Andersen *et al.*, 2004; Baker *et al.*, 2005; Simberloff, 2005). The use of imprecise data often leads to considerable uncertainty in the final risk estimates (Andrews *et al.*, 2004; Koch *et al.*, 2009). Because risk maps are used to inform decision-making, the proper representation of uncertainty is critically important (Morgan & Henrion, 1990; Gigerenzer, 2002). In general, decision-makers responsible for managing introductions of unwanted organisms are risk averse (i.e. they prefer the more certain course of action from two alternative choices with equal expected values; Shefrin & Belotti, 2007). Experts also tend to misjudge uncertainty by a considerable margin (Kahneman *et al.*, 1982). Hence, risk maps that do not incorporate uncertainty – thus placing the burden on decision-makers to address uncertainty implicitly – may lead to decision-maker overconfidence in a biased assessment. Therefore, the uncertainty associated with the estimated risk stands as an important decision variable that should be directly incorporated (i.e. by the analyst, rather than the decision-maker) into the species' risk map (Venette *et al.*, 2010). In practice, the uncertainty estimates are rarely integrated and, if addressed at all, are usually presented as a separate map (Koch *et al.*, 2009; Yemshanov *et al.*, 2009a), which decision-makers may ignore or find confusing.

Our goal with this paper was to compare a set of quantitative methods for combining an estimate of pest arrival risk and its uncertainty in a single product (so that the uncertainty cannot be ignored) and, just as importantly, to consider how the identified methods relate to the preferences and priorities of decision-makers tasked with the management of invasive species.

METHODS

Applying portfolio valuation techniques to map risks of ecological invasions

The decision-making trade-off between the estimated threat of invasion and the uncertainty in that estimate is remarkably similar to the problem of identifying an 'efficient' portfolio set in financial asset allocation. In our case, the likelihood that an invasive pest of interest will arrive at a previously uninvaded location can be seen as analogous to the concept of 'net return' in financial asset valuation, while the uncertainty of that probability estimate is, in turn, analogous to the concept of 'volatility' (Arrow, 1971; Elton & Gruber, 1996). We consider each map element as an individual 'portfolio' with an associated distribution of estimated risks of invasion. In portfolio allocation, the usual objective is to narrow down a theoretically infinite set of portfolio combinations to the fewest possible choices (an 'efficient set') that have the best trade-offs between net returns and their volatilities (Elton & Gruber, 1996). In our pest risk mapping scenario, the 'efficient' set represents the worst combination of the estimated invasion risk and the uncertainty of that estimate. Because each map element is treated as an individual portfolio, the total number of portfolios is equal to the number of elements in the map. The risk mapping problem can then be envisioned as akin to a portfolio selection strategy: the highest-risk areas in the map can be delineated by finding an 'efficient set' of 'portfolios' (individual map elements).

Under classical portfolio theory, allocation usually aims to define a single most efficient set of portfolios (Ingersoll, 1987; Elton & Gruber, 1996). A single set is sufficient because it is assumed that any investment amount can be allocated simply in specified proportions to the set of portfolios. However, allocation of resources in ecological pest management is somewhat more complex, often including financial or personnel constraints that may be poorly characterized during the risk analysis process. Thus, a goal of our risk mapping study is to provide an analysis incorporating risk and uncertainty for every map element. This was accomplished by delineating nested 'efficient' sets for all map elements. First, we evaluated the distributions of invasion risk at all n map elements comprising our study area to find a subset, $\aleph_1$, among n locations with the worst combinations in terms of projected invasion risk and its uncertainty (in short, $\aleph_1$ is analogous to the 'efficient set' in financial asset allocation terms). Once the first efficient set $\aleph_1$ was found, it was assigned the highest-risk rank 1 and removed from set n temporarily. Next, a second efficient subset, $\aleph_2$, was determined from the rest of the map, $n-\aleph_1$, assigned a rank of 2, and so forth. The process was repeated until all map elements had been evaluated and assigned a risk rank. Conceptually, this technique is similar to algorithms for finding nested non-dominated sets (Goldberg, 1989) and multi-attribute frontiers (Yemshanov *et al.*, 2010, in press).

Ecological invasion model

The portfolio allocation technique required estimating measures of projected likelihood of invasion and its uncertainty at each map element. We generated these measures with a stochastic invasion model. Spatial stochastic models have

been increasingly used for assessing risks of ecological invasions (Rafoss, 2003; Muirhead *et al.*, 2006; Cook *et al.*, 2007; Pitt *et al.*, 2009; Prasad *et al.*, 2010; Potts *et al.*, 2013) and the movement of invasive organisms in the transport networks (Robinet *et al.*, 2009; Carrasco *et al.*, 2010). Here, we applied a stochastic model that predicted the human-mediated movement of invasive forest pests through a transportation network linking major and minor settlements across Canada. In short, volumes of transported cargoes typically associated with invasive forest pests were modelled using a system of pathways through which an invader is likely to be moved (Yemshanov *et al.*, 2012a,b). The model did not consider local spread of pests by biological means, instead focusing on movement through the road network. Indeed, our choice of a pathway-based model was aimed to emphasize the importance of human-assisted spread over long distances, a phenomenon that many ecological dispersal models cannot predict well (see Andow *et al.*, 1990; Buchan & Padilla, 1999; Melbourne & Hastings, 2009).

The movement of traded commodities has been recognized as a reasonable predictor of the human-mediated spread of invasive pests (Tatem *et al.*, 2006; Hulme *et al.*, 2008; Floerl *et al.*, 2009; Hulme, 2009). We used a Commercial Vehicle Survey (CVS) maintained by Transport Canada (Yemshanov *et al.,* 2012a,b) as our primary data source. The CVS database stores summaries of individual commercial freight shipment routes (i.e. involving commodities associated with forest pests) collected during a 2005–2007 survey at truck weigh stations across Canada. A full description of the database and the pathway model can be found in the study by Yemshanov *et al.* (2012a) (see also Appendix S1 in Supporting information); here, we summarize only the model details germane to this study.

Essentially, the model represents an $n \times n$ pathway matrix where each matrix element defines the probability, p_{ij}, of an invasive forest pest being moved with commercial truck transport from one location, i, to another, j (see Appendix S1 in Supporting information). The set of locations in the pathway matrix included ≈3000 major municipalities in Canada and the United States.

We used the pathway matrix (Appendix S1 in Supporting information) to generate stochastic realizations of potential movements of a hypothetical pest of interest through the transportation network. Starting from each point of 'origin' i, the model simulated the subsequent movements of the pest from i to other locations j by extracting the associated vector of probabilities p_{ij} from the pathway matrix and using it to select the next pathway point. The process continued until the chosen node had no outgoing paths or a terminal state was selected based on the pathway matrix (Appendix S1 in Supporting information). Finally, a rate of pest arrival was estimated from the number of the times the pest arrived at j from i over the multiple stochastic pathway realizations:

$$\phi_{ij} = J_i/K \quad (1)$$

where J_i is the number of individual pathway simulations where the pest was introduced at location i and arrived at location j, and K is the total number of individual simulations of pathway spread from i ($K = 2 \times 10^6$ for each point i). The values of ϕ_{ij} were estimated for each (i, j) pair of 'origin-destination' nodes, requiring a total of K $[\phi_{ij}(\phi_{ij}-1)]$ pathway simulations.

The results were then rearranged so each j 'destination' location in the road transportation network was characterized by a distribution, ψ_j, of the pest arrival rates ϕ_{ij}, from all other nodes i, $i \neq j$. Essentially, this distribution described the location's *invasibility,* that is, the risk that it will receive a forest pest with commercial freight transported from elsewhere. Because the distribution at each potential destination point represents a multitude of arrival rate estimates from different types of origin locations, then the uncertainty in this distribution depends on the configuration of the pathway network and the levels of the transportation flows along particular pathway segments; in short, the uncertainty derives from variability in the underlying network model and data, rather than the stochasticity of the individual Monte Carlo draws during the pathway simulations. Note that these distributions do not represent uncertainty associated with a lack of knowledge about a given pest of interest. Furthermore, our exploration of the uncertainty in the arrival rates assumes that the topology of the transportation network is known in general terms.

In order to generate a spatially continuous geographic coverage, we further aggregated the location-based (i.e. point-based) arrival rate values into area-based estimates. Thus, each cell in a 15 × 15-km gridded map across Canada was characterized by a distribution of $n-1$ pest arrival rates, ψ_j, from other locations in North America. We then used these distributions to build risk maps via portfolio allocation techniques.

Basic portfolio allocation techniques

We examined two basic portfolio allocation techniques that employ, respectively, the concepts of mean-variance (M-V) frontier (Markowitz, 1952; Arrow, 1971) and second-degree stochastic dominance (SSD; Porter, 1978; Levy, 1998). We also compared these allocation techniques with a simple metric calculated as the weighted sum of the mean risk estimate and its variance [a certainty equivalent (CE); Gerber & Pafumi, 1998].

Mean-variance frontiers

The M-V concept is a visually appealing technique that, in our pest risk mapping context, plots all map cells in the dimensions of the mean risk value ($\bar{\psi}_j$, the average rate of pest arrival, across all simulations, for a map cell j) and the standard deviation of that estimate, $\sigma(\psi_j)$, which serves as a measure of uncertainty (Fig. 1a). The points, and corresponding map cells, in the outermost boundary of this

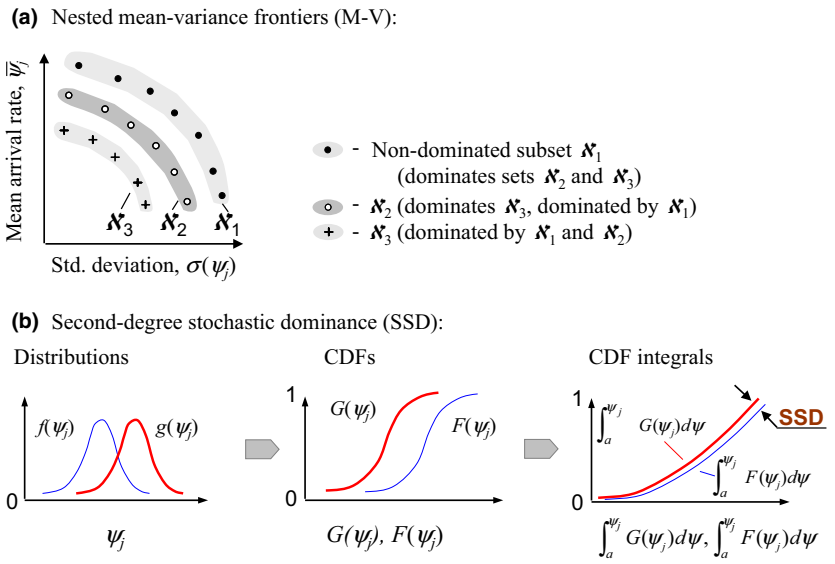

Figure 1 The concepts of nested multi-attribute mean-variance frontiers and stochastic dominance: (a) ranking risk of invasion via nested multi-attribute frontiers in dimensions of mean arrival rate and its variance; (b) comparing two distributions of invasion risk, ψ_j, via the SSD rule: $f(\psi_j)$ and $g(\psi_j)$ are example distributions of pest arrival rates at two corresponding map locations, f and g; $F(\psi_j)$ and $G(\psi_j)$ are the cumulative distribution functions (CDFs) of $f(\psi_j)$ and $g(\psi_j)$; $\int_a^{\psi_j} F(\psi_j)d\psi$ and $\int_a^{\psi_j} G(\psi_j)d\psi$ are the integrals of the CDFs. The 'SSD' label highlights a key second-order stochastic dominance condition (i.e. $\int_a^{\psi_j} F(\psi_j)d\psi$ and $\int_a^{\psi_j} G(\psi_j)d\psi$ do not cross each other).

two-dimensional cloud [i.e. comprising a convex frontier with the worst combinations of $\bar{\psi}_j$ and $\sigma(\psi_j)$] are classified as the highest risk (i.e. assigned a risk rank of 1). Then, the points in this outermost boundary of the M-V cloud are removed and the estimation proceeds inward until all points are evaluated and assigned a corresponding risk rank (Fig. 1a). Note that this delineation differs from applications of the M-V concept in economic literature, which typically identify the innermost convex boundary of lowest variance and highest net returns (Arrow, 1971; Elton & Gruber, 1996).

Stochastic dominance

The stochastic dominance (SD henceforth) concept is a form of stochastic ordering that compares a pair of distributions. The concept has been previously applied to compare the distributions of portfolio returns in financial asset valuation (Hanoch & Levy, 1969; Rothschild & Stiglitz, 1970) and shares many aspects with the partial ordering of vectors (Whitemore & Findlay, 1978; Levy, 1992).

The SD rule compares two distributions based on their cumulative distribution functions, or CDFs (Levy, 1998). In our case, we compare two risk map locations, f and g. At each location, the assemblage of plausible invasion outcomes is described by the distribution, $f(\psi_j)$ or $g(\psi_j)$, of the pest arrival rate ψ_j over an interval $[a;b]$, $\psi_j \geq 0$, $a = 0$ and $b = 1$ (Fig. 1b). The SD test compares the distributions at f and g as represented by their respective CDFs, $F(\psi_j) = \int_a^{\psi_j} f(\psi_j)d\psi$ and $G(\psi_j) = \int_a^{\psi_j} g(\psi_j)d\psi$. Location f dominates g by the first-degree stochastic dominance rule (FSD) if

$$\begin{aligned} &G(\psi_j) - F(\psi_{ij}) \geq 0 \text{ for all } \psi_j \text{ and} \\ &G(\psi_j) - F(\psi_j) > 0 \text{ for at least one } \psi_j \end{aligned} \quad (2)$$

The FSD rule implies that the CDFs of f and g do not cross each other (Fig. 1b). In practice, differences between $G(\psi_j)$ and $F(\psi_j)$ can be small, which causes the FSD conditions to fail. Alternatively, SSD provides weaker but more selective discrimination by comparing the integrals of the CDFs for $F(\psi_j)$ and $G(\psi_j)$: $\int_a^{\psi_j} F(\psi_j)d\psi$ and $\int_a^{\psi_j} G(\psi_j)d\psi$. Location f dominates the alternative g by SSD if

$$\begin{aligned} &\int_a^{\psi_j} [G(\psi_j) - F(\psi_j)]d\psi \geq 0 \text{ for all } \psi_j \text{ and} \\ &\int_a^{\psi_j} [G(\psi_j) - F(\psi_j)]d\psi > 0 \text{ for at least one } \psi_j \end{aligned} \quad (3)$$

The SSD condition implies that the integrals of the CDFs for $F(\psi_j)$ and $G(\psi_j)$ do not cross (Fig. 1b). Because $G(\psi_j)$ and $F(\psi_j)$ represent the entire distributions of estimated pest arrival rates at locations f and g, uncertainty in the ψ_j values may cause the dominance conditions to fail and therefore becomes a part of the comparison process. Importantly, the SSD rule satisfies the assumption that the decision-maker is risk averse: given two choices with the same expected (mean) value, the more certain choice is always preferred (Levy, 1998; Levy & Levy, 2001).

Our risk mapping study analysed the set of n map elements via multiple SSD tests. Each test evaluated the distributions of the area-based pest arrival rates ψ_j at two geographic locations (i.e. two map cells) f and g. Based on multiple pairwise SSD comparisons of map elements, we then delineated a non-dominant subset $\aleph_1$ from the total set n such that each element of $\aleph_1$ could not be dominated by any element in the rest of the set, $n-\aleph_1$ (according to the SSD rule, equation 3). Basically, $\aleph_1$ is equivalent to an 'efficient set' in asset allocation literature (Porter *et al.*, 1973; Fishburn & Vickson, 1978; Porter, 1978; Post & Versijp, 2007). After the first non-dominant subset $\aleph_1$ was found, assigned a risk rank of 1 and removed from set n, the next non-dominant subset was found, assigned a risk rank of 2 and so on until all elements of n were evaluated.

The delineation of nested efficient subsets is a sequential process, which we undertook in two directions. The

'top-down' approach delineated the non-dominant subsets ℵ starting from the map cells with the highest estimated risk of invasion (i.e. with the highest values from their ψ_j distributions). The bottom-up approach used the inverted ψ_j values and started the delineation of the subsets ℵ from the locations with the lowest risk and identified the highest-risk areas through step-by-step elimination of the lower-risk domains. Note that in both cases, the CDFs were integrated in ascending order starting from the lowest value in the CDF (i.e. from a to ψ_j in equations 2 and 3); hence, the dominance relationships in either case satisfy a risk-averse choice (Gasbarro *et al.*, 2009).

Certainty equivalent

The CE is a comparatively simple metric that is a weighted sum of mean risk values $\bar{\psi}_j$ and their variance $\sigma^2(\psi_j)$ for each map cell j (Gerber & Pafumi, 1998):

$$CE_j = -(\bar{\psi}_j + k\alpha\sigma^2(\psi_j)) \quad (4)$$

where $\bar{\psi}_j$ is the mean pest arrival rate (the minus sign assumes the impact of the pest's arrival is negative), k is a weighting coefficient, α is the degree of a decision-maker's risk aversion, and $\sigma^2(\psi_j)$ is the variance of the arrival rate values. Here, we examine the CE approach with k value set to 1 (i.e. with no weighting) and the $\bar{\psi}_j$ and $\sigma^2(\psi_j)$ values rescaled to a [0; 1] interval. Because information about the degree of decision-makers' risk aversion is often unavailable in pest management situations, we set the α value to 1. Note that the other method of risk-averse prioritization (i.e. the SSD rule) used in this study did not require an explicit specification of the degree of risk aversion; hence, the possible variation in α was not considered here.

Comparing the risk allocation techniques

We compared the risk ranks generated with the four aforementioned techniques (M-V, the top-down and bottom-up SSD rules, and CE) using the outputs of the stochastic invasion model (i.e. the distributions of the pest arrival rates at each map location j). To compare the results, we inverted and rescaled the risk ranks (or values, in the case of CE) generated by all techniques to a 0–1 range, so the ranks denoting the highest risk were close to 1 and the lowest risks were close to 0 (Fig. 2 and Appendix S2 in Supporting information). We then explored the impact of uncertainty by plotting the rescaled risk ranks, r_j, in the dimensions of the mean arrival rate value, $\bar{\psi}_j$, and its standard deviation, $\sigma(\psi_{ij})$ (Fig. 3).

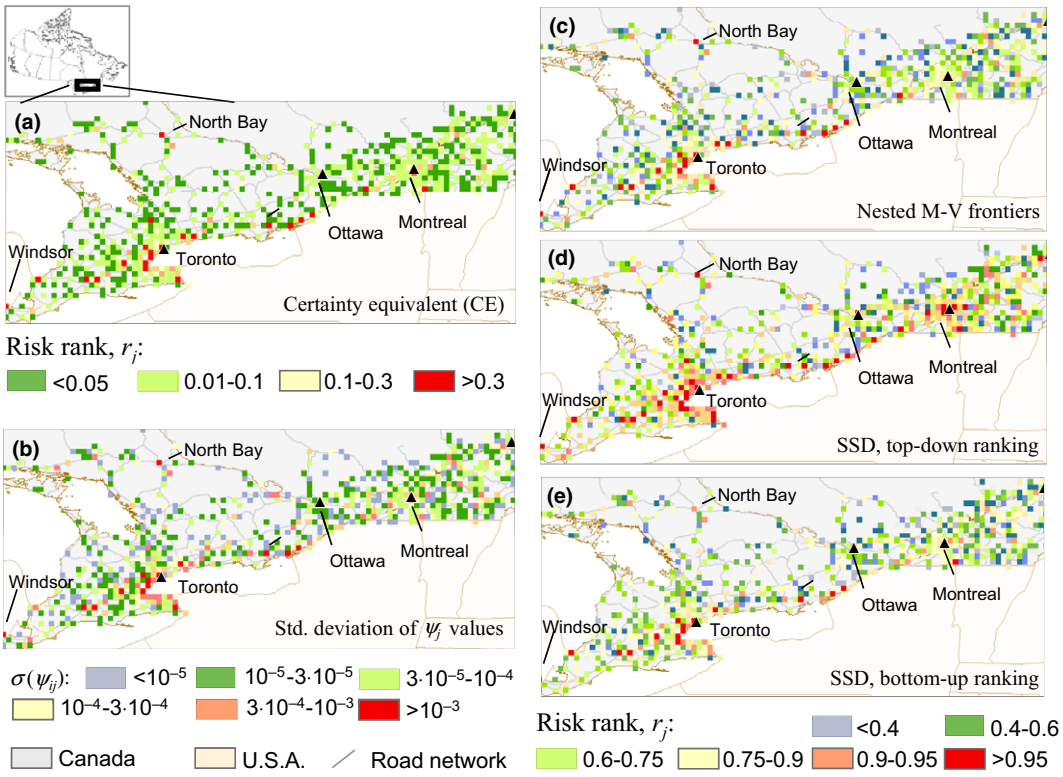

Figure 2 A comparison of risk delineations based on the certainty equivalent (CE), standard deviation of the pest arrival rate, nested mean-variance frontiers (M-V) and the stochastic dominance rule [top-down and bottom-up second-degree stochastic dominance (SSD)]. The maps show a portion of eastern Canada with the highest risk estimates. To better compare the geographic allocations of high- and low-risk areas, the map legends of the standard deviation and CE ranks were adjusted to resemble the colour palettes of the M-V and SSD maps.

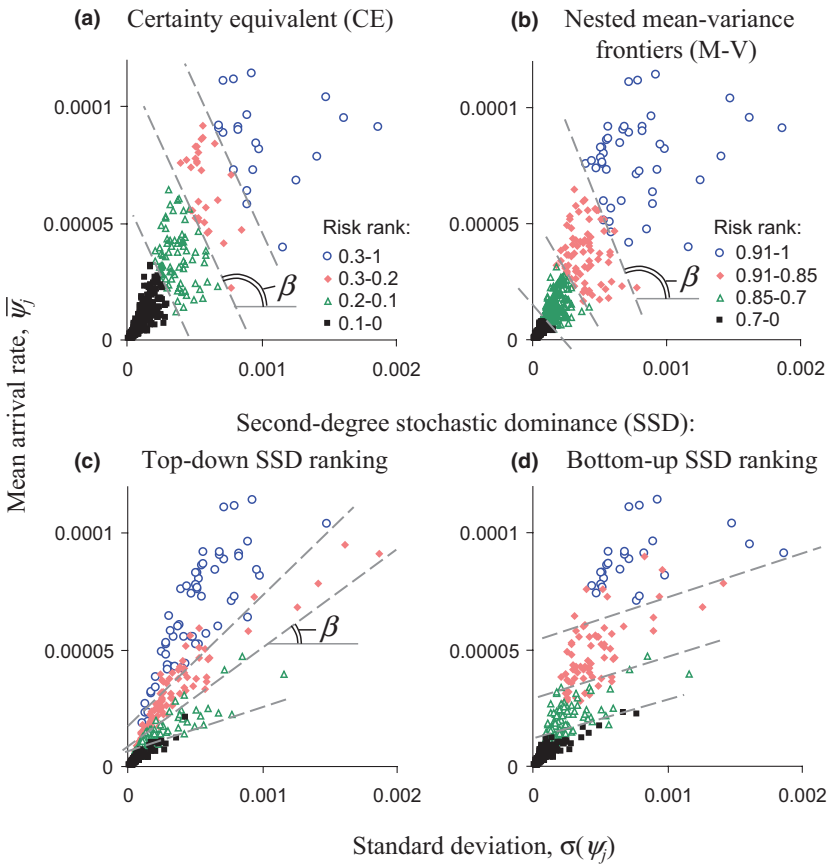

Figure 3 The rescaled risk ranks, r_i, in dimensions of the mean pest arrival rate, $\bar{\psi}_j$, and its standard deviation, $\sigma(\psi_j)$. β denotes the tilt angle between the boundaries of risk classes in the mean-variance cloud and the line indicating constant mean arrival rate (ψ_j = const). The levels of broad risk classes in the second-degree stochastic dominance (SSD) classifications (different symbol types in c and d) are similar to the symbol levels in the mean-variance (M-V) classification (see legend in b).

Estimating the risk ranking errors

We estimated the standard error of the rescaled risk ranks, $\mathrm{se}(r_j)$, via bootstrap and jackknife tests. These tests were used to evaluate two different sources of error. Bootstrapping estimates the sampling distribution of a population by generating new samples via drawing (with replacement) from the original data (Efron & Tibshirani, 1993). Alternatively, jackknifing estimates the error by computing the risk ranks for n combinations of the data where one of the original elements (map cells) is removed (a leave-one-out jackknife; Shao & Tu, 1995).

The bootstrapping test involved simulating, for each map location j, B independent bootstrap samples with replacement of size n where each independent value of ψ_j (i.e. the distribution of arrival rate values for j) was sampled with the probability $1/n$. For each bootstrap sample, we then recalculated the rescaled risk ranks, $r^*_{j\mathrm{boot}}$, using the M-V and SSD approaches. The bootstrap standard error was estimated as

$$\mathrm{se}(r_j)_{\mathrm{boot}} = \sqrt{\frac{1}{B-1}\sum_{1}^{B}\left(r^*{}_{j\,\mathrm{boot}} - \bar{r}^*{}_{j\,\mathrm{boot}}\right)^2}, \quad \text{where } \bar{r}^*{}_{j\,\mathrm{boot}} = \frac{1}{B}\sum_{1}^{B} r^*{}_{j\,\mathrm{boot}} \tag{5}$$

The bootstrap used here involves resampling arrival rates from different model runs. Thus, $\mathrm{se}(r_j)_{\mathrm{boot}}$ gives a measure of the variability in rank for map location j that is due to using a finite number of model runs, rather than a hypothetical infinite set composed of all possible model runs.

In the jackknife test, for each map location j, we generated n samples of size $n-1$ by leaving out one location at a time and recalculating the rescaled ranks, $r^*_{j\mathrm{jack}}$. The standard error was calculated as

$$\mathrm{se}(r_j)_{\mathrm{jack}} = \sqrt{\frac{n-1}{n}\sum_{1}^{n}\left(r^*{}_{j\,\mathrm{jack}} - \bar{r}^*{}_{j\,\mathrm{jack}}\right)^2}, \quad \text{where } \bar{r}^*{}_{j\,\mathrm{jack}} = \frac{1}{n}\sum_{1}^{n} r^*{}_{j\,\mathrm{jack}} \tag{6}$$

The jackknife used here involves resampling from map locations. Thus, $\mathrm{se}(r_j)_{\mathrm{jack}}$ gives a measure of the variability in rank for map location j that is due to a change in the network configuration.

To understand how relative rank related to these two sources of variability, we plotted the bootstrap and jackknife standard errors against the r_j values. For consistency, we used the same number of resamples in both tests (i.e. $B = n$).

RESULTS

Broad-scale geographic risk patterns

Appendix S2 depicts the nationwide geographic pattern of risk ranks across Canada based on the top-down SSD rule. The

map generally highlights how Canada's major transportation arteries serve as key pathways for new pest arrivals. For example, in eastern Canada, the areas labelled as moderate to high risk ($r_j > 0.75$) are associated with major transportation hubs in Ontario and Quebec: municipalities located along the Highway 401 corridor between the Detroit (MI)-Windsor (ON) area and Montreal (QC). Moreover, although most of the arrival hotspots are located in eastern Canada (Appendix S2, a), one noteworthy region in western Canada is the greater Vancouver area (BC), extending to the nearby border crossing with the United States (Appendix S2, b).

Figure 2 compares maps of risk ranks based on the CE, M-V and SSD rules (both top-down and bottom-up approaches) with a map of the standard deviation, $\sigma(\psi_j)$, of the arrival rate values. All ranking methods provided similar delineations of the highest-risk areas (Fig. 2). Among the portfolio-based classifications (i.e. based on the SSD and M-V rules), the top-down SSD delineation showed the largest number of high-risk ranks above 0.9 (Fig. 2d). The high-risk areas delineated by all three portfolio-based classifications (Fig. 2c–e) were typically areas with high variability in ψ_j (represented by high $\sigma(\psi_j)$ values; see Fig. 2b).

Table 1 lists major municipalities that were assigned a top-20 risk rank by at least one ranking method (shaded cells in Table 1). The top-20 lists generated with the M-V and SSD methods are different from the ranks based on the mean arrival rate ($\bar{\psi}_j$) and the CE. For example, five locations in the top-20 lists for the M-V and SSD delineations – Iroquois (ON), Moncton (NB), Drummondville (QC), Trois-Rivieres (QC) and Sainte-Madeleine (QC) – had considerably lower ranks in the classifications based on the CE and the mean arrival rate. Because the probabilistic pathway model considered only forest-pest-associated commodities transported via the road network, not all major Canadian municipalities appeared in the list of the highest ranks. For example, large cities such as Edmonton (AB), Vancouver (BC) and Saskatoon (SK) had moderate-risk ranks, $r_j < 0.85$.

Risk ranks in dimensions of the mean arrival rate and its standard deviation

Uncertainty figures prominently in the delineations based on the M-V and SSD rules (Fig. 2). This is evident when the rescaled risk ranks, r_j, for individual map cells are plotted in the dimensions of mean pest arrival rate ($\bar{\psi}_j$) and its standard deviation, $\sigma(\psi_{ij})$ (Fig. 3). Different symbols in Fig. 3 delineate broad classes of risk ranks: 0–0.7, 0.7–0.85, 0.85–0.91 and 0.91–1 for the M-V and SSD delineations and 0–0.1, 0.1–0.2, 0.2–0.3 and 0.3–1 for the CE ranks.

The CE approach delineated the boundaries between these risk rank classes as parallel planes at equal intervals (dashed lines in Fig. 3a). The boundaries between the risk classes in Fig. 3a were always tilted at an angle, β, above 90 degrees (which means that a location with the same mean arrival rate as another location, but higher variability, will receive a higher-risk rank). The boundaries between ranks delineated with the M-V rule were similarly tilted at $\beta > 90°$, but they were not parallel as in the CE approach; instead, their angles were uniquely influenced by the local density of points in the M-V cloud. This behaviour is expected: because the M-V ranks are delineated as nested two-attribute (M-V) frontiers (Fig. 1a), the adjacent M-V frontiers are expected to be much closer to each other when passing through a high-point-density area than through a low-point-density area. Note also that the delineation of the M-V ranks starts from the outermost upper part of the M-V point cloud, which explains the tilt angle above 90 degrees.

For the delineations based on the SSD rule, the tilt angle β of the boundaries between the risk classes was below 90° (Fig. 3c, d). This implies that between two locations with equal mean arrival rates, the location with the more certain estimate (i.e. with lower variability) would be assigned a higher rank. There are also noteworthy differences in the risk ranks delineated by the top-down and bottom-up SSD approaches. As described previously, in the top-down SSD approach (Fig. 3c), the ranking process started from locations with the highest pest arrival rates, whereas the bottom-up SSD approach (Fig. 3d) started ranking from the locations with the lowest arrival rates. In turn, the two approaches are similar in terms of the highest- and lowest-ranked locations, but for moderate-risk ranks, the methods appear to place differing levels of emphasis on certainty in the arrival rate estimate (i.e. the top-down approach seems to be less tolerant of high variability). This distinctive behaviour occurs because the sequential delineation of the non-dominant subsets proceeds differently under the top-down or bottom-up rules. Errors tend to accumulate in the direction by which the delineation proceeds, which causes characteristic changes in the structure of the remaining non-dominant subsets. Fundamentally, the non-dominance conditions under which either the top-down or bottom-up rule is applied to a set may not be symmetric. Briefly, if subset, *A,* of a set *N* is non-dominant to the rest of the set, *N*', this does not always imply that when the values in *N* are inverted, the subset *N*' would be non-dominant to subset *A*.

The disparate treatment of uncertainty in the M-V- and SSD-based algorithms can be further illustrated by the pattern of differences in their rank values. Figure 4 depicts the rank values for map locations generated with the M-V (*x*-axis) and top-down SSD rules (*y*-axis). The magnitude of differences between the M-V and SSD ranks increases gradually as the rank value increases from zero and peaks in the middle rank values between 0.4 and 0.6. This pattern is influenced by the shapes of the arrival rate distributions. In the case of a normally distributed variable, the M-V efficient set would be the same as the SSD-efficient set for a decision-maker who is risk averse. However, the delineation of M-V frontiers in our example started from the upper outermost boundary of the M-V cloud. Also, for multimodal and skewed distributions that fail the test for normality, mean values and variance estimates may not describe the distribution adequately, so the estimated ranks under the M-V algorithm could be lower (or higher) than under SSD.

Table 1 A comparison of 'top-20' locations ranked by different allocation methods

Location name (aggregated to the nearest largest municipality)	Province*	Location type†	Risk allocation method‡								
			$\bar{\psi}_j$	CE		M-V		SSD			
								Top-down		Bottom-up	
			Relative rank§	$r_{j\ CE}$§	Relative rank*	$r_{j\ M\text{-}V}$	Relative rank	$r_{j\ FSD}$	Relative rank	$r_{j\ SSD}$	Relative rank
Highest-risk municipalities (Top-20 locations identified by at least one risk ranking method)											
Cornwall	ON	UB	14¶	0.23	16	**1.0**	1	**1.0**	1	**1.0**	1
Toronto	ON	U	1	**0.96**	1	**1.0**	2	**1.0**	1	**0.99**	2
Windsor (ON)	ON	UB	3	0.37	7	**0.98**	4	**1.0**	1	**0.98**	4
Kitchener	ON	U	9	0.31	10	**0.99**	3	**0.99**	6	**0.98**	3
Drummondville	QC	U	39	0.12	43	**0.98**	5	**0.98**	11	**0.97**	5
Trois-Rivieres	QC	U	30	0.15	32	**0.97**	7	**0.99**	7	**0.95**	7
Iroquois	ON	T	45	0.09	53	**0.96**	8	**0.99**	5	**0.94**	8
Quebec	QC	U	34	0.12	40	**0.93**	15	**1.0**	1	**0.90**	17
Moncton	NB	U	28	0.15	36	**0.97**	6	**0.98**	10	**0.96**	6
Sainte-Madeleine	QC	T	22	0.17	25	**0.95**	10	**0.99**	8	**0.93**	11
Montreal	QC	U	15	0.21	21	**0.95**	9	**0.98**	9	**0.94**	9
Sarnia	ON	UB	6	0.28	13	**0.94**	13	**0.97**	14	**0.92**	13
Lacolle	QC	TB	52	0.07	64	**0.94**	11	**0.97**	12	**0.93**	10
Hamilton	ON	U	16	0.21	20	**0.92**	18	**0.97**	13	0.89	19
London	ON	U	4	0.41	6	**0.94**	12	**0.96**	19	**0.92**	12
Saint-Georges	QC	UB	73	0.05	75	**0.93**	16	**0.96**	16	**0.91**	15
Napanee	ON	U	10	0.33	9	**0.92**	17	**0.95**	23	**0.91**	16
Windsor (QC)	QC	T	42	0.15	35	**0.91**	22	**0.96**	17	0.90	18
North Bay	ON	U	19	0.22	17	**0.92**	19	**0.95**	24	**0.91**	14
Ottawa	ON	UB	38	0.11	47	0.88	32	**0.96**	18	0.86	36
Gananoque	ON	UB	2	0.47	3	**0.91**	20	**0.94**	32	0.89	20
Nobleton	ON	T	80	0.03	108	0.86	45	**0.96**	15	0.88	22
Oshawa	ON	U	5	0.33	8	0.89	26	**0.94**	31	0.84	44
Calgary	AB	U	8	0.45	5	**0.94**	14	0.90	56	0.86	29
Sorel	QC	U	89	0.04	88	0.86	41	**0.96**	20	0.86	34
White Rock	BC	UB	7	0.47	2	**0.91**	21	0.89	60	0.88	23
Niagara Falls	ON	UB	13	0.24	15	0.87	33	**0.93**	34	0.88	24
Sault Ste. Marie	ON	UB	20	0.21	22	0.86	40	**0.92**	42	0.87	26
Abbotsford	BC	UB	11	0.47	4	**0.91**	23	0.88	68	0.86	33
Kingston	ON	U	18	0.22	19	0.88	31	**0.91**	47	0.88	25
Sparwood	BC	T	24	0.25	14	0.90	25	0.86	76	0.85	41
Orono	ON	T	17	0.22	18	0.85	50	**0.92**	44	0.86	35
Ingersoll	ON	T	12	0.31	11	0.87	36	0.89	63	0.86	30
Thunder Bay	ON	U	27	0.29	12	0.86	44	0.79	140	0.82	58
Other notable cities											
Halifax	NS	U	102	0.03	129	0.86	42	**0.93**	36	0.84	47
Winnipeg	MB	U	32	0.14	37	0.88	30	**0.91**	49	0.85	40
Sudbury	ON	U	36	0.12	41	0.85	48	0.88	65	0.86	32
Edmonton	AB	U	35	0.18	24	0.84	54	0.85	87	0.84	45
Vancouver	BC	U	43	0.15	31	0.83	57	0.84	96	0.85	27
Barrie	ON	U	21	0.19	23	0.82	63	0.83	103	0.86	28
Saskatoon	SK	U	75	0.06	67	0.82	70	0.81	125	0.85	37
Lethbridge	AB	U	123	0.03	109	0.77	104	0.78	146	0.85	38
Regina	SK	U	167	0.01	182	0.75	119	0.77	150	0.83	53
Fredericton	NB	U	194	0.01	214	0.69	165	0.81	122	0.83	51

*Canadian provinces: AB – Alberta; BC – British Columbia; MB – Manitoba; NB – New Brunswick; NS – Nova Scotia; ON – Ontario; QC – Quebec; SK – Saskatchewan.

†Location type: U – urban area; B – border crossing with the United States.; T – town.

‡Risk allocation method: $\bar{\psi}_j$ – based on the mean arrival rate value; CE – based on the certainty equivalent; M-V – based on nested mean-variance frontiers; SSD – based on the second-degree stochastic dominance rule (top-down and bottom-up ranking approaches).

§Risk metric: r_j – location-specific risk rank rescaled to a 0–1 range.

'relative rank' – the location's order rank in the table based on the r_j value.

¶The top 20 relative ranks are shaded in grey; the risk rank values $r_j > 0.9$ are outlined in boldface.

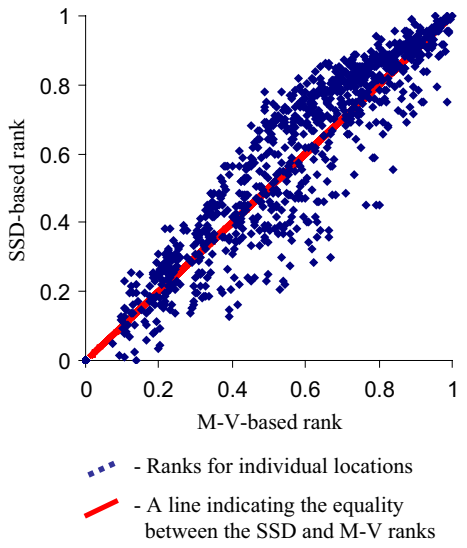

Figure 4 Risk rankings in the second-degree stochastic dominance (SSD) classification versus the mean-variance (M-V) classifications. *X*-axis shows the rescaled risk rank in the M-V scenario, and *y*-axis shows the rescaled rank in the SSD scenario. A 45° line shows the positions where the M-V and SSD-based ranks are equal.

Estimates of ranking errors

Figure 5a, c and e shows minimum, median and maximum bootstrap standard errors, $se(r_j)_{boot}$, plotted against the rescaled risk rank values, r_j, for the three ranking methods. Becausethe ranking methods based on nested non-dominant frontiers (i.e. the M-V and SSD rules) tend to accumulate errors as the ranking proceeds from highest- towards lowest-risk ranks (or, in the case of the bottom-up SSD rule, from lowest to highest), we depicted basic trends in errors as a function of the rank value. The standard errors represent the variability in rank due to the use of a finite number of model runs to approximate the 'true' distribution of arrival times. The ranks based on the M-V rule had the largest errors, with median $se(r_j)_{boot}$ approaching 0.12 (Fig. 5a). The top-down SSD ranking had the lowest errors, with median $se(r_j)_{boot}$ below 0.05 (Fig. 5c). The bootstrap errors for the bottom-up SSD ranking were higher, but median $se(r_j)_{boot}$ remained below 0.08 (Fig. 5e).

For the SSD top-down technique (Fig. 5c), errors were the lowest for the highest ranks ($r_j > 0.85$), which were delineated first and then displayed an increase in variability for ranks between 0.15 and 0.85. Overall, the errors remained relatively low, as indicated by the nearly straight, gently sloping lines for median $se(r_j)_{boot}$. The median errors generated with the SSD bottom-up technique were generally higher, especially for the moderate rank values between 0.55 and 0.8. Compared to the top-down SSD classification, the maximum bootstrap error values for the range of ranks between 0.15 and 0.6 (Fig. 5e, dashed line) were also higher.

In general, the delineations based on convex M-V frontiers (Fig. 5a, b) showed higher errors than the methods based on pairwise SSD tests. Because the nested efficient

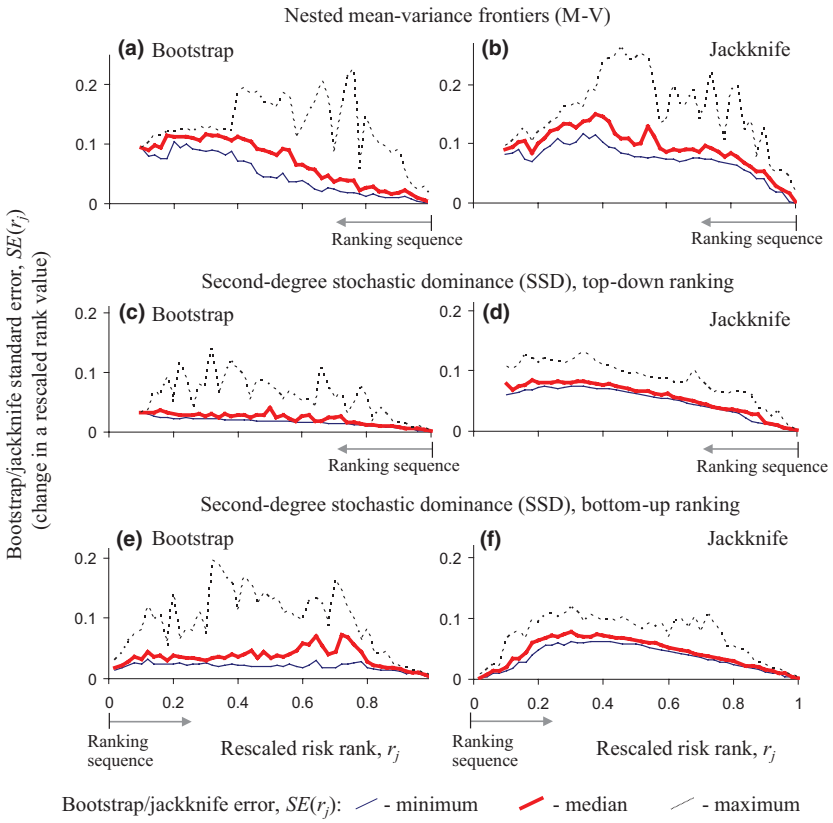

Figure 5 Bootstrap and jackknife standard errors of the risk ranks, r_j. *X*-axis denotes the rescaled risk value; the standard error in the *y*-axis is the change in the rescaled rank value. Arrow denotes the starting point and direction of the successive delineation of nested non-dominant frontiers (i.e. starting from the highest ranks towards lowest in the mean-variance (M-V) and top-down second-degree stochastic dominance (SSD) classifications, and from the lowest to the highest ranks in the bottom-up SSD classification).

sets in the SSD or M-V classifications were delineated in sequential order, the standard errors were the lowest for the ranks delineated first. For all three methods, errors increased in a fairly linear fashion in the direction of the ranking sequence. With respect to the bottom-up SSD classification, the errors were also very low for the ranks above 0.9 (i.e. at the end of the ranking sequence for this approach, with fewer locations left to rank and more apparent differences between the remaining locations). Overall, then, the bootstrap standard errors indicate that, at least for high- and moderate-risk ranks above 0.7, the top-down SSD classification was least influenced by the use of a finite number of model runs in the analysis, although bottom-up SSD also performed similarly for high-risk locations above 0.8.

Figure 5b, d and f shows, respectively, the jackknife standard errors for the ranks delineated with the M-V, top-down SSD and bottom-up SSD approaches. Compared to the bootstrap estimates, the median error values were considerably higher. This is logical: the removal of an element from a non-dominant set during the jackknife tests may change the dominance relationships between the other elements. The minimum–maximum error ranges in Fig. 5 also help understand the general variation of the ranking errors. Because the jackknife test did not employ resampling with replacement, the location-to-location variation of the error values in the SSD-based classifications was lower than in the bootstrap test, so the minimum–maximum ranges in Fig. 5d and f appear to be narrower and more uniform than in the M-V approach (Fig. 5b).

DISCUSSION

The portfolio-based techniques appear to be dependable risk mapping methods when prior knowledge about an invasive organism is imprecise. Both the M-V and the SSD techniques delineated nested 'efficient' sets of map elements based on a partial order of these elements in a space defined by the invasion model outputs (i.e. the mean arrival rate and its standard deviation in the M-V scenario, and distributions of invasion risks in the form of CDF integrals in the SSD scenario). Their reliance on a partial order of elements makes these approaches fairly robust to errors in data and model assumptions about the organism of interest. Because the SSD and M-V non-dominant sets are discrete, it takes a higher degree of uncertainty to alter the partial ordering of elements (i.e. the arrangement of points in M-V space, or the dominance relationships in the SSD scenario) in these scenarios and move a particular point from one non-dominant set to another. However, the CE method uses a continuous weighted summation, so any small alteration in the mean arrival rate or its variance changes the resulting rank value linearly.

The techniques presented offer a strategy for dealing with the typical lack of knowledge about an invasive organism (which commonly translates into a problem of combining a multitude of differing assessments into a one-dimensional risk estimate and generating consistent rankings based on imprecise data). Furthermore, this lack of knowledge often causes experts to generate fairly coarse assessments in vague 'high–low' terms. Although experts can discern the meaningful trends in the predicted outcome of an invasion, they are rarely able to assign precise probability values. In the portfolio-based techniques, each geographic location is ordered along a 'high–low' risk gradient by finding nested 'efficient' sets, which makes the issue of assigning precise values less critical.

Note that the M-V rule assumes that the first two distribution moments (i.e. the mean and the variance) provide an adequate representation of the distribution as a whole (Gandhi & Saunders, 1981). This may preclude the application of the method in many practical situations where the distribution fails the test for normality. Alternatively, the stochastic dominance approach evaluates the entire cumulative distribution of expected outcomes and does not require testing the distribution for normality (Fishburn & Vickson, 1978).

Incorporating the decision-maker's risk preferences

The risk mapping techniques based on the CE, M-V and the SSD rules depict two decision-making strategies that offer different treatments of uncertainty. The CE and M-V rules may be suitable in situations when uncertainty about the organism of interest is considered as a factor that could potentially increase the level of priority for decision-makers. This situation is common in risk assessments aimed to aid early detection of invasive organisms, when the need to gain more information about the invader is paramount.

Alternatively, a delineation based on the SSD rule may be more suitable for assessments that support costly decisions (such as restricting trade or imposing a regulation) or when a decision-maker otherwise shows risk-averse preferences with respect to the chosen risk metric. While the SSD rule operates from the perspective that a decision-maker is fundamentally risk averse (Porter *et al.*, 1973; Levy, 1998; Meyer *et al.*, 2005), it does not require an explicit specification of a degree of risk aversion or defining a numerical 'utility' value for every possible invasion outcome that a decision-maker may encounter. Furthermore, if the risk metric (or the 'utility' value) takes into account costs or is represented in a monetary equivalent (*cf.* Hauser & McCarthy, 2009; Hester *et al.*, 2013), then the SSD rule could be applied to these metrics to prioritize cost-effective management actions in spatially heterogeneous environments. It is also common for decision-makers to focus on a certain range of risk values. If the delineation of highest-risk sites is the main objective, then the top-down SSD ranking approach is suitable. When the decision-making objective is to identify and filter off the lowest-risk domains (which will not require any action), a bottom-up SSD ranking method would be a better choice.

Ultimately, the applicability of a particular risk prioritization method can be affected by the choice of the risk metric used in the assessment. The choice of metric may change the

interpretation of the uncertainty associated with the metric's variation and subsequently demand a different risk ranking method. For example, when a risk assessment is intended to assist with pest surveillance (i.e. to provide new information about the distribution of a pest), the modelled probability of pest arrival is not sufficient to characterize the potential information gain from, for example, an unexpected detection of the pest in a low-probability location. In such a case, the uncertainty of the arrival rate estimates becomes a distinctly important variable, and so the prioritization would best be done in the two dimensions of the arrival rate and its variance. The use of the M-V algorithm would seem appropriate in this instance. Furthermore, one could estimate the risk ranks with all three proposed algorithms and then order map locations in a three-dimensional space using multicriteria aggregation techniques that do not require setting the criteria weights (such as the multi-attribute frontier aggregation described in Yemshanov *et al.*, in press).

Computational remarks

The M-V and SSD techniques use somewhat different methods to generate the risk ranks. The M-V approach 'peels' the cloud of points (representing individual map locations) in dimensions of the mean risk and its variance, starting from the outermost layer (Fig. 1a). Alternatively, the stochastic dominance approach ranks the geographic locations via multiple pairwise SSD tests (Fig. 1b). As a consequence, the two techniques typically yield different numbers of elements at the highest-risk ranks. Typically, the M-V approach generates a larger number of elements in the outermost frontiers (as is evident from Fig. 1a). The allocation of the frontiers in the M-V approach can also be influenced by local variations of the point density in the M-V space: more frontiers can be delineated in regions of the M-V space with higher point density. This may explain the considerably higher ranking errors estimated for the M-V approach in the bootstrap and jackknife tests.

ACKNOWLEDGEMENTS

The authors extend their gratitude and thanks to Kirsty Wilson and Marty Siltanen (Natural Resources Canada, Canadian Forest Service) for technical support and diligence with preparing the case study dataset for this study. The participation of Denys Yemshanov was supported by an interdepartmental NRCan – CFIA Forest Invasive Alien Species initiative. The participation of Mark Ducey was supported by the Agriculture and Food Research Initiative Competitive Grants Program Grant No. 2010-85605-20584 from the National Institute of Food and Agriculture.

REFERENCES

Andersen, M.C., Adams, H., Hope, B. & Powell, M. (2004) Risk assessment for invasive species. *Risk Analysis*, **24**, 787–793.

Andow, D.A., Kareiva, P.M., Levin, S.A. & Okubo, A. (1990) Spread of invading organisms. *Landscape Ecology*, **4**, 177–188.

Andrews, C.J., Hassenzahl, D.M. & Johnson, B.B. (2004) Accommodating uncertainty in comparative risk. *Risk Analysis*, **24**, 1323–1335.

Arrow, K.J. (1971) *Essays in the theory of risk bearing*. Markham, Chicago.

Baker, R., Cannon, R., Bartlett, P. & Barker, I. (2005) Novel strategies for assessing and managing the risks posed by invasive alien species to global crop production and biodiversity. *The Annals of Applied Biology*, **146**, 177–191.

Boender, G.J., Hagenaars, T.J., Bouma, A., Nodelijk, G., Elbers, A.R.M., de Jong, M.C.M. & van Boven, M. (2007) Risk maps for the spread of highly pathogenic avian influenza in poultry. *PLoS Computational Biology*, **3**, e71.

Borchert, D., Fowler, G. & Jackson, L. (2007) *Organism pest risk analysis: risks to the conterminous United States associated with the Woodwasp, Sirex noctilio* Fabricius, and the symbiotic fungus, *Amylostereum areolatum*, (Fries: Fries) Boidin. USDA-APHIS-PPQ-CPHST-PERAL. 2007. Rev.1. Available at: http://www.aphis.usda.gov/plant_health/plant_pest_info/sirex/downloads/sirex-pra.pdf (accessed 30 March 2009).

Briggs, D. (2000) *Environmental health hazard mapping for Africa*. Report Commissioned by WHO-AFRO, Harare, Zimbabwe. Available at: http://www.emro.who.int/ceha/pdf/healthhazard.pdf (accessed 20 Feb 2012).

Buchan, L.A.J. & Padilla, D.K. (1999) Estimating the probability of long-distance overland dispersal of invading aquatic species. *Ecological Applications*, **9**, 254–265.

Büchele, B., Kreibich, H., Kron, A., Thieken, A., Ihringer, J., Oberle, P., Merz, B. & Nestmann, F. (2006) Flood-risk mapping: contributions towards an enhanced assessment of extreme events and associated risks. *Natural Hazards and Earth System Sciences*, **6**, 485–503.

Carrasco, L.R., Mumford, J.D., MacLeod, A., Harwood, T., Grabenweger, G., Leach, A.W., Knight, J.D. & Baker, R.H.A. (2010) Unveiling human-assisted dispersal mechanisms in invasive alien insects: integration of spatial stochastic simulation and phenology models. *Ecological Modelling*, **221**, 2068–2075.

Cook, D.C., Thomas, M.B., Cunningham, S.A., Anderson, D.L. & De Barro, P.J. (2007) Predicting the economic impact of an invasive species on an ecosystem service. *Ecological Applications*, **17**, 1832–1840.

Efron, B. & Tibshirani, R.J. (1993) *An introduction to the bootstrap*. Chapman and Hall, New York, NY.

Elton, E.J. & Gruber, M.J. (1996) *Modern portfolio theory and investment analysis*, 5th edn. Wiley, New York, NY.

Fishburn, P.C. & Vickson, R.C. (1978) Theoretical foundations of stochastic dominance. *Stochastic dominance. An approach to decision-making under risk* (ed. by G.A. Whitemore and M.C. Findlay), pp. 39–144. Lexington Books, D.C. Heath and Co., Lexington, MA.

Floerl, O., Inglis, G.J., Deym, K. & Smith, A. (2009) The importance of transport hubs in stepping-stone invasions. *Journal of Applied Ecology*, **46**, 37–45.

Gandhi, D.K. & Saunders, A. (1981) The superiority of stochastic dominance over mean variance efficiency criteria: some clarifications. *Journal of Business Finance & Accounting*, **8**, 51–59.

Gasbarro, D., Wong, W.-K. & Kenton, Z.J. (2009) *Stochastic dominance and behavior towards risk: the market for iShares*. Available from http://ssrn.com/abstract=1365756 (accessed 12 December 2011).

Gerber, H.U. & Pafumi, G. (1998) Utility functions: from risk theory to finance. *North American Actuarial Journal*, **2**, 74–100.

Gigerenzer, G. (2002) *Calculated risks: how to know when numbers deceive you*. Simon & Schuster, New York, NY.

Goldberg, D.E. (1989) *Genetic algorithms in search, optimization, and machine learning*. Addison-Wesley Publ. Co., Reading, MA.

Hanoch, G. & Levy, H. (1969) The efficiency analysis of choices involving risk. *Review of Economic Studies*, **36**, 335–346.

Hauser, C.E. & McCarthy, M.A. (2009) Streamlining 'search and destroy': cost-effective surveillance for invasive species management. *Ecology Letters*, **12**, 683–692.

Hester, S.M., Cacho, O.J., Panetta, F.D. & Hauser, C.E. (2013) Economic aspects of post-border weed risk management. *Diversity and Distributions*, **19**, 580–589.

Hulme, P.E. (2009) Trade, transport and trouble: managing invasive species pathways in an era of globalization. *Journal of Applied Ecology*, **46**, 10–18.

Hulme, P.E., Bacher, S., Kenis, M., Klotz, S., Kuhn, I., Minchin, D., Nentwig, W., Olenin, S., Panov, V., Pergl, J., Pysek, P., Roques, A., Sol, D., Solarz, W. & Vila, M. (2008) Grasping at the routes of biological invasions: a framework for integrating pathways into policy. *Journal of Applied Ecology*, **45**, 403–414.

Ingersoll, J.E. Jr (1987) *Theory of financial decision making*. Rowman & Littlefield, Lanham, MD.

Kahneman, D., Slovic, P. & Tversky, A. (eds.) (1982) *Judgment under uncertainty: heuristics and biases*. Cambridge University Press, NY, New York.

Koch, F.H., Yemshanov, D., McKenney, D.W. & Smith, W.D. (2009) Evaluating critical uncertainty thresholds in a spatial model of forest pest invasion risk. *Risk Analysis*, **29**, 1227–1241.

Koch, F.H., Yemshanov, D., Colunga-Garcia, M., Magarey, R.D. & Smith, W.D. (2011) Establishment of alien-invasive forest insect species in the United States: where and how many? *Biological Invasions*, **13**, 969–985.

Levy, H. (1992) Stochastic dominance and expected utility: survey and analysis. *Management Science*, **38**, 555–593.

Levy, H. (1998) *Stochastic dominance: investment decision making under uncertainty*. Kluwer Academic Publishers, The Netherlands.

Levy, M. & Levy, H. (2001) Testing for risk aversion: a stochastic dominance approach. *Economics Letters*, **71**, 233–240.

Magarey, R.D., Colunga-Garcia, M. & Fieselmann, D.A. (2009) Plant biosecurity in the United States: roles, responsibilities, and information needs. *BioScience*, **59**, 875–884.

Magarey, R.D., Borchert, D.M., Engle, J.S., Colunga-Garcia, M., Koch, F.H. & Yemshanov, D. (2011) Risk maps for targeting exotic plant pest detection programs in the United States. *OEPP/EPPO Bulletin*, **41**, 1–11.

Markowitz, H. (1952) Portfolio selection. *The Journal of Finance*, **7**, 77–91.

Melbourne, B.A. & Hastings, A. (2009) Highly variable spread rates in replicated biological invasions: fundamental limits to predictability. *Science*, **325**, 1536–1539.

Meyer, T., Xiao-Ming, L. & Rose, L.C. (2005) Comparing mean variance tests with stochastic dominance tests when assessing international portfolio diversification benefits. *Financial Services Review*, **14**, 149–168.

Morgan, M.G. & Henrion, M. (1990) *Uncertainty: a guide to dealing with uncertainty in quantitative risk and policy analysis*. Cambridge University Press, New York, NY.

Muirhead, J.R., Leung, B., van Overdijk, C., Kelly, D.W., Nandakumar, K., Marchant, K.R. & MacIsaac, H.J. (2006) Modelling local and long-distance dispersal of invasive emerald ash borer *Agrilus planipennis* (Coleoptera) in North America. *Diversity and Distributions*, **12**, 71–79.

Pitt, J.P.W., Worner, S.P. & Suarez, A.V. (2009) Predicting Argentine ant spread over the heterogeneous landscape using a spatially explicit stochastic model. *Ecological Applications*, **19**, 1176–1186.

Porter, R.B. (1978) Portfolio applications: empirical studies. *Stochastic dominance. An approach to decision-making under risk* (ed. by G.A. Whitemore and M.C. Findlay), pp. 117–162. Lexington Books, D.C. Heath and Co., Lexington, MA.

Porter, R.B., Wart, J.R. & Ferguson, D.L. (1973) Efficient algorithms for conducting stochastic dominance tests on large numbers of portfolios. *Journal of Financial and Quantitative Analysis*, **8**, 71–81.

Post, T. & Versijp, P. (2007) Multivariate tests for stochastic dominance efficiency of a given portfolio. *Journal of Financial and Quantitative Analysis*, **42**, 489–515.

Potts, J.M., Cox, M.J., Barkley, P., Christian, R., Telford, G. & Burgman, M.A. (2013) Model-based search strategies for plant diseases: a case-study using citrus canker (*Xanthomonas citri*). *Diversity and Distributions*, **19**, 590–602.

Prasad, A.M., Iverson, L.R., Peters, M.P., Bossenbroek, J.M., Matthews, S.N., Syndor, T.D. & Schwartz, M.W. (2010) Modeling the invasive emerald ash borer risk of spread using a spatially explicit cellular model. *Landscape Ecology*, **25**, 353–369.

Rafoss, T. (2003) Spatial stochastic simulation offers potential as a quantitative method for pest risk analysis. *Risk Analysis*, **23**, 651–661.

Robinet, C., Roques, A., Pan, H., Fang, G., Ye, J., Zhang, Y. & Sun, J. (2009) Role of human-mediated dispersal in the spread of the pinewood nematode in China. *PLoS ONE*, **4**, e4646.

Rothschild, M. & Stiglitz, J.E. (1970) Increasing risk. I. A definition. *Journal of Economic Theory*, **2**, 225–243.

Shao, J. & Tu, D. (1995) *The Jackknife and bootstrap*. Springer, New York, NY.

Shefrin, H. & Belotti, M.L. (2007) *Behavioral finance: biases, mean-variance returns, and risk premiums*. CFA Institute Publications, New York, NY, June 2007, 4–12

Simberloff, D. (2005) The politics of assessing risk for biological invasions: the USA as a case study. *Trends in Ecology & Evolution*, **20**, 216–222.

Tatem, A.J., Rogers, D.J. & Hay, S.I. (2006) Global transport networks and infectious disease spread. *Advances in Parasitology*, **62**, 293–343.

US Department of Agriculture, Forest Health Technology Enterprise Team (FHTET). (2007a) *Sirex woodwasp risk maps*. Available at: http://www.fs.fed.us/foresthealth/technology/invasives_sirexnoctilio_riskmaps.shtml (accessed 12 June 2010).

US Department of Agriculture, Forest Health Technology Enterprise Team (FHTET). (2007b) *Sirex woodwasp – sirex noctilio. Methods*. Available at: http://www.fs.fed.us/foresthealth/technology/pdfs/SirexIntroductionSummary.pdf http://www.fs.fed.us/foresthealth/technology/pdfs/SirexEstablishmentSummary.pdf (accessed 20 July 2010).

US Federal Emergency Management Agency (FEMA). (2003) *Guidelines and specifications for flood hazard mapping partners*. Available at: http://www.fema.gov/library/viewRecord.do?id=2206 (accessed 20 Dec 2011).

Venette, R.C., Kriticos, D.J., Magarey, R., Koch, F.H., Baker, R.H.A., Worner, S.P., Gómez, N.N., McKenney, D.W., Dobesberger, E.J., Yemshanov, D., De Barro, P.J., Hutchison, W.D., Fowler, G., Kalaris, T.M. & Pedlar, J. (2010) Pest risk maps for invasive alien species: a roadmap for improvement. *BioScience*, **60**, 349–362.

Whitemore, G.A. & Findlay, M.C. (1978) Introduction. *Stochastic dominance. An approach to decision-making under risk* (ed. by G.A. Whitemore and M.C. Findlay), pp. 1–36. Lexington Books, D.C. Heath and Co., Lexington, MA.

Yemshanov, D., Koch, F.H., McKenney, D.W., Downing, M.C. & Sapio, F. (2009a) Mapping invasive species risks with stochastic models: a cross-border United States-Canada application for *Sirex noctilio* Fabricius. *Risk Analysis*, **29**, 868–884.

Yemshanov, D., McKenney, D.W., De Groot, P., Haugen, D.A., Sidders, D. & Joss, B. (2009b) A bioeconomic approach to assess the impact of a nonnative invasive insect on timber supply and harvests: a case study with *Sirex noctilio* in eastern Canada. *Canadian Journal of Forest Research*, **39**, 154–168.

Yemshanov, D., Koch, F.H., Ben-Haim, Y. & Smith, W.D. (2010) Detection capacity, information gaps and the design of surveillance programs for invasive forest pests. *Journal of Environmental Management*, **91**, 2535–2546.

Yemshanov, D., Koch, F.H., Lyons, B., Ducey, M. & Koehler, K. (2012a) A dominance-based approach to map risks of ecological invasions in the presence of severe uncertainty. *Diversity and Distributions*, **18**, 33–46.

Yemshanov, D., Koch, F.H., Ducey, M. & Koehler, K. (2012b) Trade-associated pathways of alien forest insect entries in Canada. *Biological Invasions*, **14**, 797–812.

Yemshanov, D., Koch, F.H., Ben-Haim, Y., Downing, M. & Sapio, F. (2013) A new multi-criteria risk mapping approach based on a multi-attribute frontier concept. *Risk Analysis*. doi: 10.1111/risa.12013

SUPPORTING INFORMATION

Additional Supporting Information may be found in the online version of this article:

Appendix S1 A probabilistic pathway model of invasive species movement with commercial freight transport through a North American transportation network.

Appendix S2 The geographic distribution of the rescaled risk ranks, r_i, across Canada (only the top-down SSD delineation is shown, see Fig. 2 for a comparison with other ranking techniques).

BIOSKETCH

Denys Yemshanov is a research scientist in the Canadian Forest Service at Natural Resources Canada. His research specialization can be described as development of spatial models focused on various ecological and bioeconomic aspects of forest resources. Areas of his special interest include the development of risk modeling and mapping techniques and impact models for invasive alien species. His resent work is focused on modeling pathways of human-assisted spread of invasive alien species with international trade, commercial transportation and recreational travel in the North America.

Author contributions: Lead: concept for the study; development and programming of the SSD, M-V and CE ranking algorithms and the probabilistic pathway model; undertaking numeric simulations and error tests; development of the first draft – D.Y.; Linking the problem of human-assisted spread of invasive pests with the commercial transportation and commodity flow contexts; linking the pathway model with the commodity flow network data; discussion of main results – F.K and D.Y.; Discussion on the theoretical foundations and performance of the SSD, M-V and CE algorithms, and the bootstrap and jackknife tests – M.D. Expertise with the Canadian roadside survey database, identification of pest-associated commodities in the dataset – K.K. All authors contributed to the writing and editing of the manuscript.

Editor: Mark Burgman